

Tricritical directed percolation in 2+1 dimensions

Peter Grassberger

John-von-Neumann Institute for Computing, Forschungszentrum Jülich, D-52425 Jülich, Germany

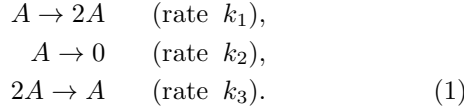
(Dated: June 7, 2018)

We present detailed simulations of a generalization of the Domany-Kinzel model to 2+1 dimensions. It has two control parameters p and q which describe the probabilities P_k of a site to be wetted, if exactly k of its “upstream” neighbours are already wetted. If P_k depends only weakly on k , the active/adsorbed phase transition is in the directed percolation (DP) universality class. If, however, P_k increases fast with k so that the formation of inactive holes surrounded by active sites is suppressed, the transition is first order. These two transition lines meet at a tricritical point. This point should be in the same universality class as a tricritical transition in the contact process studied recently by Lübeck. Critical exponents for it have been calculated previously by means of the field theoretic epsilon-expansion ($\epsilon = 3 - d$, with $d = 2$ in the present case). Rather poor agreement is found with either.

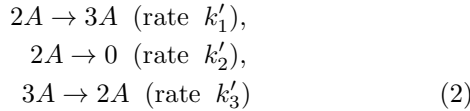
I. INTRODUCTION

The critical behaviour of directed percolation (DP) has been studied since more than 30 years, if we also count the work on ‘reggeon field theory’ [1] which was only later recognized as a field theory for a stochastic process which is in the DP universality class [2]. In spite of this long history, several of its aspects have barely received any attention yet. In particular this is true for its tricritical version.

DP is e.g. realized by a reaction-diffusion system



Its mean field theory is just the rate equation for the number $n(t)$ of A particles, $\dot{n} = an - bn^2$ with $a = k_1 - k_2$ and $b = k_3$. The transition is in this description at $a = 0$. The first mentioning of tricritical DP (TDP) seems to have been made in this context by [3], where it was pointed out that the system composed of the reactions



has the rate equation

$$\dot{n} = bn^2 - cn^3 \quad (3)$$

with $b = k'_1 - 2k'_2$, $c = k'_3$. This is just the mean field equation for a system with tricritical point at

$$b = 0, \quad c > 0. \quad (4)$$

But, as observed by Janssen [4] and Ohtsuki & Keyes [5], Eqs.(3) and (4) can be realized also differently, e.g. by combining both reaction-diffusion systems and choosing $k_1 - k_2 = 0$, $k'_1 - 2k'_2 - k_3 = 0$, $k'_3 > 0$.

Both versions differ however beyond the mean field level, if fluctuations are taken into account. While the

combination of Eqs.(1) and (2) should be described by a Langevin equation $\dot{n}(\mathbf{x}, t) = an(\mathbf{x}, t) + bn^2(\mathbf{x}, t) - cn^3(\mathbf{x}, t) + \xi(\mathbf{x}, t)$ with the “semi-multiplicative” noise, $\langle \xi(\mathbf{x}, t)\xi(\mathbf{x}', t') \rangle \propto n(\mathbf{x}, t)\delta(\mathbf{x} - \mathbf{x}')\delta(t - t')$, well known from reggeon field theory, the noise appropriate for Eq.(2) alone should be particle number conserving when $n \rightarrow 0$, i.e. [6] $\langle \xi(\mathbf{x}, t)\xi(\mathbf{x}', t') \rangle \propto n^2(\mathbf{x}, t)\delta(\mathbf{x} - \mathbf{x}')\delta(t - t') + \text{const } n(\mathbf{x}, t)\nabla^2\delta(\mathbf{x} - \mathbf{x}')\delta(t - t')$.

The reaction scheme Eq.(2) has become infamous during the last years as “pair contact process with diffusion” (PCPD) [7], and has received very much attention. It is still basically unsolved [8]. In contrast, there was no activity on the “true” tricritical DP with semi-multiplicative noise, after Ohtsuki & Keyes had worked out the lowest order results of the ϵ -expansion. This has changed only very recently with field theory work by Janssen [9] and with extensive and careful simulations by Lübeck [10].

The present work was mainly started because only the stationary behaviour was studied in [10], and we wanted to obtain also dynamical (tri-)critical exponents. It seems that the dynamical behaviour of TDP was never studied numerically before. Indeed, for ordinary DP it is also easier to obtain static critical exponents from dynamical simulations than from stationary behaviour. Although this might be different for TDP, it seems worth to check it. But we made also a few other changes. In particular we study a model with parallel updating in discrete time, while a model with continuous time (the tricritical ‘contact process’ [11] instead of TDP proper) was studied in [10]. These two models should be in the same universality class, but a check would be welcome – and simulating discrete time processes is often faster. Finally, while the exponents observed in [10] were rather close to the mean field values, some of them deviated from mean field theory in the opposite direction of that predicted by the ϵ -expansion. Simulating a different model in the same universality class with emphasis on different aspects might clarify whether this indicates a failure (or slow convergence) of the ϵ -expansion, or hints at problems with the simulations.

In this paper, we study a fully discrete model which

is actually a generalization of the well known Domany-Kinzel (DK) model [12]) to 2+1 dimensions. This generalization to higher dimensions is necessary, because there is no non-trivial tricritical point in 1+1 dimensions (the cross over to the first order transition, called “compact DP” [13] in this case, happens at the boundary of the DK phase diagram, just as the phase transition in the 1-d Ising model occurs at $T = 0$ [14]. At the tricritical point we obtain rather precise estimates of the (tri-)critical exponents, except for the cross-over exponent which is affected by large corrections to scaling. Beyond this point, when the active/adsorbed transition is first order, we find that clusters starting with single sites survive with a stretched exponential probability. This is similar to the decay of clusters in the Grassberger-Chaté-Rousseau (GCR) model with re-infection easier than first infection [15, 16], and has a similar qualitative reason [17]. The boundary between active and adsorbed regions behaves, near the first order transition, like a generic fluctuating non-equilibrium (KPZ [18]) surface and shows the same scaling laws.

In the next section we will define the model and describe some special features of the simulations. Predictions to compare our simulations with are reviewed in Sec.3. Results will be presented in Sec.4, while the paper end with a discussion in Sec.5.

II. THE GENERALIZED DOMANY-KINZEL MODEL

The standard DK model lives on a square lattice. Usually, this lattice is drawn as tilted by 45° , and a site can be wetted by its two lower neighbours. For a more easy later generalization to 2+1 dimensions, we use a non-tilted lattice, so that site $(x, t+1)$ can be wetted by sites $(x-1, t)$ and $(x+1, t)$. The probability to be wetted is $P_1 = y$, if one of these sites was wetted, and $P_2 = z$, if both were wetted. Here y and z are real numbers between 0 and 1. If $y = z$, this corresponds to site DP, while bond DP corresponds to $z = y(2-y)$. If $y < 1/2$, any finite cluster of active (=wetted) sites dies with probability one. For any $y > 1/2$, there is a second order phase transition (in the DP universality class) to a surviving active phase at $z = z_c(y)$. Finally, when $y = 1/2$ the cluster dies still with probability one, but the average life time is infinite when $z = 1$. This is then the case of compact DP [13].

In 2+1 dimensions we take a square lattice in space, and each site $(\mathbf{x}, t+1)$ can be infected by any of the four sites $(\mathbf{x} \pm \mathbf{e}_1, t)$, $(\mathbf{x} \pm \mathbf{e}_2, t)$. Assuming still that at least one of these sites has to be active in order to activate $(\mathbf{x}, t+1)$, we have now four wetting (“infection”, “activation”) probabilities P_k , $k = 1, 2, 3, 4$. Site percolation corresponds to $P_k = p$ for all k , while bond percolation corresponds to $P_1 = p$, $P_{k+1} = P_k + (1 - P_k)p$ for $k > 1$. These formulas are easily understood: In site percolation it does not matter how many of the neighbours are active, since the site will be wetted anyhow, if it can be wetted

at all. In bond percolation, the chance to be wetted by $k+1$ neighbours is equal to the chance that the first k of them succeeded, plus the chance that the last one succeeds if the first were unsuccessful. We have thus 4 control parameters, but generically it will be sufficient to study a 2-dimensional subspace. We choose (somewhat arbitrarily) the following 2-parametric ansatz

$$P_1 = p, \quad P_{k+1} = P_k + (1 - P_k)pq \quad \text{for } k > 1 \quad (5)$$

with $0 < p < 1$ and q such that all P_k are positive and less than 1. This ansatz includes both site DP ($q = 0$) and bond DP ($q = 1$). When $0 < q < 1/p$, it has a similar interpretation to the one given for bond DP: if the first k attempts were all unsuccessful in wetting the site, the chance for the next one is not p but is qp . But Eq.(5) is independent of this interpretation and is legitimate also for $q < 0$, provided $0 \leq P_k \leq 1$ for all k .

Simulations of this model are straightforward. At each time t we have two lists L_{old} and L_{new} of sites, together with an integer array S of size $L \times L$, where L is the linear size of the system. At the beginning we put $t = 0$, S and L_{new} are empty, and L_{old} contains the coordinates of the seed (we use helical boundary conditions, i.e. each site is labelled by a single integer i with $i \equiv i + L^2$, and its four neighbours are $i \pm 1$ and $i \pm L$). When going from t to $t+1$, we first go through the list L_{old} and increase $S[i]$ by one unit, whenever i is a neighbour of a site in L_{old} . At the same time we write each of these i into the list L_{new} . In a second pass, we first erase L_{old} , then we check which sites in L_{new} are actually wetted (for this, we use the information stored in S). Those who are wetted are written into L_{old} , and $S[i]$ is reset to zero for all checked sites. We then erase L_{new} , and are ready to go from $t+1$ to $t+2$.

There are two non-trivial tricks for improving this algorithm. The first is needed in the first order transition regime. There, the survival probabilities decay extremely fast with time t . Therefore we use enrichment, implemented recursively as in the PERM algorithm [19]. Essentially, this makes a copy of every cluster which survives up to a t where the fraction of surviving clusters is below some threshold, and lets the copy and the original evolve independently.

The second trick is related to histogram reweighting [20, 21], but it is done on the fly as in [22]. Assume a cluster contains n_k sites wetted by k neighbours ($k = 1, \dots, 4$) and b_k boundary sites which were *not* wetted, although they had k wet neighbours. Such a cluster is included in the sample with probability

$$P(\{n_k\}, \{b_k\}; p, q) = \prod_{k=1}^4 P_k^{n_k} (1 - P_k)^{b_k}. \quad (6)$$

For any observable A , the average is

$$\begin{aligned} \langle A \rangle_{p,q} &= \sum_{\{n_k\}, \{b_k\}} A(\{n_k\}, \{b_k\}) P(\{n_k\}, \{b_k\}; p, q) \\ &= M^{-1} \sum_{\text{events}} A(\{n_k\}, \{b_k\}), \end{aligned} \quad (7)$$

where the first sum runs over all possible configurations and the second sum runs over all M actually simulated clusters. The average for some other pair (p', q') of control parameters is then given by

$$\langle A \rangle_{p', q'} = M^{-1} \sum_{\text{events}} A(\{n_k\}, \{b_k\}) \frac{P(\{n_k\}, \{b_k\}; p', q')}{P(\{n_k\}, \{b_k\}; p, q)}. \quad (8)$$

The ratio of probabilities is actually calculated by multiplying the corresponding ratios of P_k resp. $1 - P_k$ for each site which is wetted (resp. not wetted) during the build-up of the cluster.

This is useful, if we want to estimate several averages during the same run. It is particularly useful, if we want to estimate derivatives of $\langle A \rangle_{p, q}$ with respect to p or q . The latter is needed for checking scaling laws, as we will discuss below. Such derivatives can be obtained directly from Eq.(8), e.g.

$$\frac{\partial}{\partial p} \langle A \rangle_{p, q} = M^{-1} \sum_{\text{events}} A(\{n_k\}, \{b_k\}) W \quad (9)$$

with

$$W = \sum_{\text{wetted sites}} \frac{\partial}{\partial p} \ln P_k(p, q) + \sum_{\text{non-wetted sites}} \frac{\partial}{\partial p} \ln(1 - P_k(p, q)). \quad (10)$$

We made several types of runs. Most extensively, we started from a single seed and measured the averages of the number $N(t)$ of sites wetted at time t , of the survival probability $P(t)$, and of the rms. distance $R^2(t)$ of wetted sites from the seed [23]. In several of these runs we also calculated reweighted averages of $N(t)$ and/or $\partial \langle N(t) \rangle / \partial p$. In addition, we made also some simulations with fully active initial conditions, where we measured the decay of the density $\rho(t)$ of sites active at time t . Finally, we made some runs also with initial conditions where half of the lattice was fully active and the other half was empty [10]. In that case one has two phase boundaries, and one can watch how these boundaries evolve with time.

In all cases, lattice sizes were sufficiently large that we have no finite size corrections. This is most easily checked in single-seed runs: One simply has to check that the wetted region never hits the boundary of the lattice. In the other cases the check is less straightforward, but we always verified that $L/2 \gg t^{1/z}$, where z is the dynamical exponent. In most cases this implied $L > 1000$ for $t \approx 40, 000$.

III. THEORETICAL PREDICTIONS

For each value of q , we expect that there is a critical value $p_c(q)$ such that the activity dies out for $p < p_c(q)$, while $\lim_{t \rightarrow \infty} P(t) > 0$ for $p > p_c(q)$. For all values of q ,

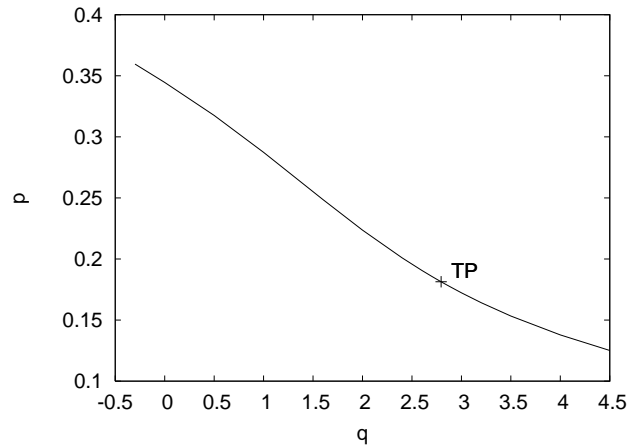


FIG. 1: Phase diagram for the generalized DK model in 2+1 dimensions. Below the transition line, activity dies out, while an active phase exists above it. The transition is in the DP universality class to the left of the tricritical point marked “TP”, while it is first order to its right. The actual locations of the curve and of the tricritical point were obtained from numerical simulations.

$p_c(q)$ is a decreasing function. Known numerical values are for $q = 0$ and $q = 1$: $p_c(0) = 0.34457(1)$ (site DP [24]) and $p_c(1) = 0.2873381(1)$ (bond DP [24, 25]). The phase diagram should thus look roughly as in Fig. 1. At the tricritical point TP: $(p, q) = (p^*, q^*)$, the observables $N(t)$, $P(t)$, $R^2(t)$, and $\rho(t)$ should follow power laws

$$N(t) \sim t^\eta (1 + O(t^{-\Delta})), \quad P(t) \sim t^{-\delta'} (1 + O(t^{-\Delta})), \\ R^2(t) \sim t^{2/z} (1 + O(t^{-\Delta})), \quad \rho(t) \sim t^{-\delta} (1 + O(t^{-\Delta})) \quad (11)$$

Here, Δ is the exponent of the leading correction to scaling term.

The upper critical (spatial) dimension is $d_c = 3$. For $d > d_c$ one has the mean field exponents $\eta = 0$, $\delta' = 1$, $z = 2$, and $\delta = 1/2$. The predictions of the ϵ -expansion with $\epsilon = 3 - d$ are [5, 9]

$$\eta = -0.0193\epsilon + O(\epsilon^2) \approx -0.019 \\ \delta' = 1 - 0.0193\epsilon + O(\epsilon^2) \approx 0.981 \\ z = 2 + 0.0086\epsilon + O(\epsilon^2) \approx 2.009 \\ \delta = \frac{1}{2} - 0.468\epsilon + O(\epsilon^2) \approx 0.032 \quad (12)$$

Here the numerical values are those obtained for $d = 2$ by simply neglecting all terms higher than linear in ϵ . These values satisfy, up to terms $O(\epsilon^2)$, the hyperscaling relation [11, 26]

$$\eta + \delta + \delta' = d/z. \quad (13)$$

To derive the latter, remark that $P(t)$ is the probability that there exists at least one path of active sites connecting the site $(\mathbf{x}_0, t_0) = (0, 0)$ to any of the sites (\mathbf{x}, t) . Similarly, $\rho(t)$ is the chance that there exists at least one

path connecting any site $(\mathbf{x}, 0)$ to $(0, t)$. The probability that $(0, 0)$ is connected to $(0, t)$ scales, according to our Ansatz for $N(t)$ and $R^2(t)$, as $P_{\text{conn}} \sim N(t)/R^d \sim t^{\eta-d/z}$. On the other hand, if there is basically at most one percolating cluster near $\mathbf{x} = 0$ (an assumption which breaks down for $d > d_c$), and if the site $(\mathbf{x}, 0)$ belongs to it, then the condition for $(0, t)$ to be wetted is the same as that for $(0, t)$ to be connected to $(0, 0)$. Thus $P_{\text{conn}} \approx P(t)\rho(t)$, which gives immediately Eq. (13).

In the vicinity of the tricritical point one should distinguish between the behaviour on the critical curve (but with $q \neq q^*$) from the behaviour off the critical curve. For the former, we expect for each observable a scaling ansatz with scaling variable $(q^* - q)t^x$, e.g. for $N(t)$ we have

$$N(t; q, p = p_c(q)) = t^\eta F((q^* - q)t^x). \quad (14)$$

Notice that it would be more standard to use $(q^* - q)^{1/x}t$ as scaling variable, but then the scaling function replacing $F(z)$ would be singular at the origin. The advantage of Eq. (14) is that $F(z)$ is analytic at $z = 0$. On the other hand, for $q = q^*$ and $p \neq p_c(q^*)$ we have [27]

$$N(t; q^*, p) = t^\eta G((p_c(q^*) - p)t^y). \quad (15)$$

Again, the standard way of writing this would be in terms of the scaling variable $(p_c(q^*) - p)^{\nu_\parallel}t$ with $\nu_\parallel = 1/y$, the advantage of Eq. (15) being that $G(z)$ is analytic at $z = 0$.

Eq. (15) shows that the correlation time scales as $\tau \propto (p_c(q^*) - p)^{\nu_\parallel}$, and therefore the correlation length scales as $\xi \propto (p_c(q^*) - p)^{\nu_\perp}$ with $\nu_\perp = \nu_\parallel/z$. The cross over exponent ϕ is finally defined as

$$\phi = x/y. \quad (16)$$

The ϵ -expansion gives [5, 9]

$$\begin{aligned} \nu_\parallel &= 1 + 0.0193\epsilon + O(\epsilon^2) \approx 1.019, \\ \phi &= \frac{1}{2} - 0.0121\epsilon \approx 0.488, \\ \nu_\perp &= \frac{1}{2} + 0.0075\epsilon \approx 0.507. \end{aligned} \quad (17)$$

Since the tricritical point TP is a fixed point of the renormalization group flow which is instable in both directions, we should slowly cross over to the scaling laws for normal DP, if we are on the transition line with $q < q^*$. Thus, normal DP asymptotics is expected on the entire transition line left of TP. For DP one has the same scaling laws Eq.(11), but with different exponents [24, 25, 28]: $\eta = 0.2303(4)$, $\delta = \delta' = 0.4509(5)$, and $z = 1.7666(10)$. These values satisfy the same hyperscaling relation Eq. (13).

The identity $\delta = \delta'$ follows from a special time reversal symmetry which holds for bond and site DP, but not for the DK model in general. As we said above, both $P(t)$ and $\rho(t)$ are probabilities that one point at the boundary of a time slice $0 \leq t' \leq t$ is connected to some point on

the opposite boundary. For bond DP one sees easily that both are the same, i.e. $\rho(t) = P(t)$ exactly. For site DP one gets the same, if one assumes also all sites with $t' = 0$ and $t' = t$ as wettable with probability p , which gives e.g. $P(1) = \rho(1) = p[1 - (1 - p)^4]$. No relation like that holds for the general DK model.

On the part of the transition line with $q > q^*$ one has compact clusters with only few small holes and a slowly moving rough surface. This is analogous to critical compact DP, except that the latter occurs (in 1+1 dimensions) only at a single point and has clusters without any holes at all. Mean field arguments [10] suggest that the transition is first order along this part, in the sense that the density of active sites in the stationary state is discontinuous. The growth of a cluster is then similar to the growth of a droplet in a usual first order phase transition, except that now one of the two phases is not fluctuating.

Consider now an initially straight interface between the two phases. If $p < p_c(q)$, this interface will move into the direction of the active phase, i.e. the inactive phase will win. The opposite is true for $p > p_c(q)$, i.e. the value of $p_c(q)$ is fixed by the condition that neither phase will win in the long time limit [10, 29, 30]. Notice, however, that this does not mean that the interface at $p = p_c(q)$ will not move during short times. Due to the asymmetry between the two phases, we expect the generic behaviour of non-equilibrium (“growing”) interfaces to apply, i.e. the velocity of the critical interface should scale with time as $v \sim t^{-2/3}$ for large t [18].

Let us finally discuss the growth of a cluster starting from a single site for $q > q^*$, $p = p_c(q)$. As in the Grassberger-Chaté-Rousseau model with negative partial immunization, it is easier to survive for the cluster in its already occupied region than to spread out from this region. Although the details of the two models are different, we might thus expect that we find also in the present model a stretched exponential law, $P(t) \sim \exp(-ct^\alpha)$, for basically the same qualitative reasons as in the Grassberger-Chaté-Rousseau model [16]. We have however no detailed prediction on the exponent α .

IV. RESULTS

A. Gross features of the phase diagram

For ordinary DP, the observable most sensitive to the precise value of p_c is $N(t)$. We expect therefore that $N(t)$ is also the best observable to locate the tricritical point. In Fig. 2 we show $N(t)$ for twelve pairs of control parameters (p, q) . These represent three values of p (critical, sub-, and supercritical) for each of four values of q . The latter are chosen to be: (i) site DP ($q = 0$); (ii) in the crossover region from TDP to DP ($q = 2.4$); (iii) close to TDP ($q \approx q^* \approx 2.8$) and (iv) $q > q^*$. First of all, we see from Fig. 2 that there are indeed two straight lines. These are of course the candidates for ordinary and for

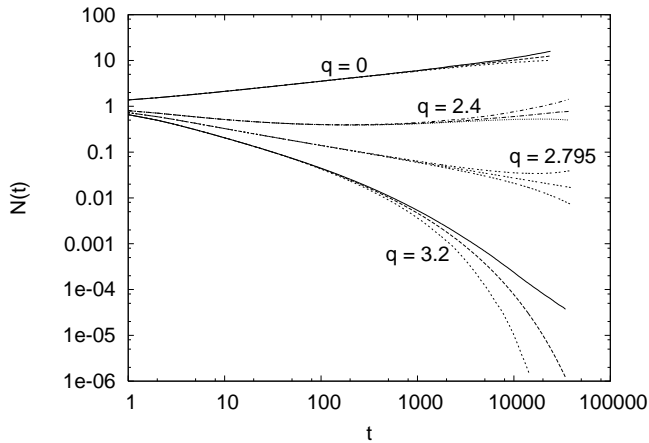


FIG. 2: Log-log plots of $N(t)$ for four different values of q , and for three values of p for each q . The three p -values are chosen to be subcritical, critical, and supercritical (bottom to top). Within each triple, they differ by less than 0.05%. The four q -values are DP, crossover from TDP to DP, TDP, and first order (top to bottom).

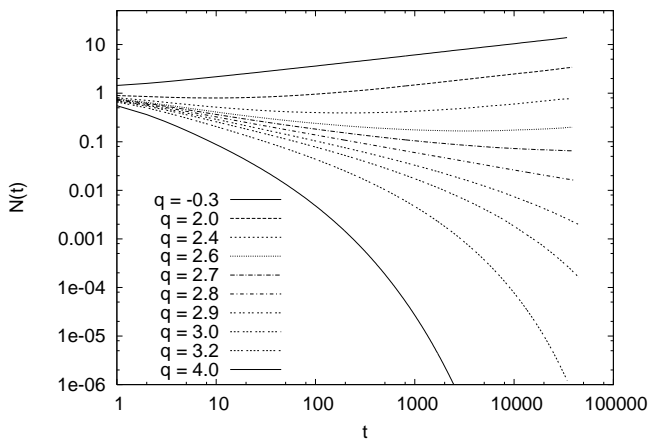


FIG. 3: Log-log plots of $N(t)$ for several values of q , each at the best estimate of $p_c(q)$.

tricritical DP. Secondly, we see that we can determine $p_c(q)$, for each value of q , with rather high precision. For $q = q^*$ we just have to look for a power law, just as for $q \ll q^*$. For q in the cross-over region, i.e. close to q^* but not at q^* , the determination of $p_c(q)$ is less easy. But we still can get rather precise estimates for q slightly below q^* , if we assume that the slopes of the critical curves approach the slope $\eta = 0.2303$ of the critical DP curve monotonously. For $q \gg q^*$, finally, it is more easy to determine $p_c(q)$ from the requirement that the velocity of a straight interface scales as $t^{-2/3}$ (see details below) than from the behaviour of $N(t)$. Numerical results for $p_c(q)$ obtained in this way are collected in Table 1. Several critical curves are plotted again in Fig. 3.

TABLE I: Estimates of $p_c(q)$.

q	$p_c(q)$	comment
-0.3	0.359568(3)	
0.0	0.344575(5)	site DP
0.5	0.317505(3)	
1.0	0.287339(2)	bond DP
1.6	0.248648(2)	
2.0	0.223647(2)	
2.40	0.200939(1)	
2.60	0.1906655(9)	
2.70	0.185809(1)	
2.75	0.1834507(9)	
2.78	0.1820572(7)	
2.79	0.1815965(4)	
2.795	0.1813672(3)	TDP
2.80	0.1811382(4)	
2.82	0.180225(1)	
2.85	0.178870(2)	
2.9	0.176648(5)	
3.0	0.172337(5)	
3.2	0.164243(4)	
3.5	0.153313(3)	
4.0	0.137830(3)	
4.5	0.12508(1)	
5.0	0.11444(1)	

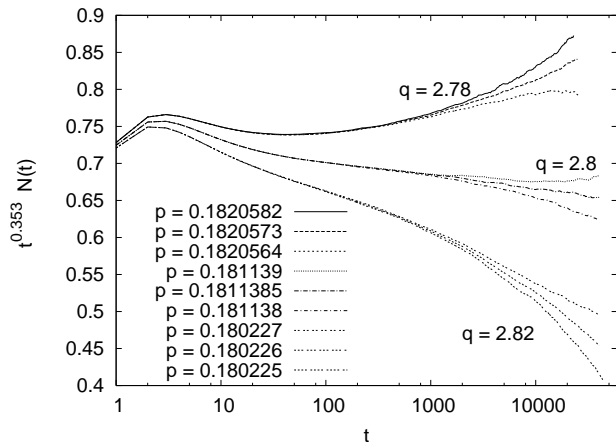


FIG. 4: Log-linear plots of $t^{-\eta}N(t)$ for several values of $q \approx q^*$ and $p \approx p_c(q)$, with $\eta = -0.353$.

B. Scaling at the tricritical point

Plots like those in Fig. 2 are of course not suitable for precise determinations of critical parameters. For a closer look at the tricritical region, we show in Fig. 4 the product $t^{-\eta}N(t)$ with $\eta = -0.353$. This value of

η is our best estimate, i.e. the tricritical curve should be horizontal if there were no corrections to the scaling behaviour. Actually we see that there are quite strong corrections, manifesting themselves as a bump at $t \approx 3$. The data shown in Fig. 2 and similar data at other nearby values of q show that

$$q^* = 2.792(6), \quad p_c = 0.1831534(5) + 0.458(2.792 - q^*), \quad (18)$$

and

$$\eta = -0.353(9). \quad (19)$$

Although the last estimate has the same sign as the prediction from the ϵ -expansion, it is larger by nearly a factor 20!

Once we have fixed the tricritical point, we can immediately obtain δ' and z from the scaling of $P(t)$ and $R^2(t)$. We do not show the corresponding data. The estimates found by standard extrapolation methods are

$$\delta' = 1.218(7), \quad z = 2.110(6). \quad (20)$$

For z we find that the deviation from the mean field value $z = 2$ has the same sign as predicted (TDP spreads subdiffusively, in agreement with the intuitive notion that spreading should be slowed down compared to ordinary DP). But again the difference from mean field is an order of magnitude larger than predicted. For the correction to δ' , the ϵ -expansion predicted even a wrong sign.

Finally, in order to measure the exponent δ , we made runs with fully active initial conditions. Again we do not show the raw data, as they contained little surprises. They give

$$\delta = 0.087(3). \quad (21)$$

In spite of the huge difference from mean field behaviour (where $\delta = 1/2$), this is in surprising good agreement with Eq. (12). The hyperscaling relation is very well satisfied with these estimates,

$$\eta + \delta + \delta' - d/z = 0.004(13), \quad (22)$$

showing that they are at least internally consistent.

C. Scaling near the tricritical point

A popular method to find correlation length and cross-over exponents are data collapse plots. In view of a scaling law like Eq. (15), it seems natural to plot $N(t)/t^\eta$ against $(p_c(q^*) - p)t^y$ and determine y (or, equivalently, ν_{\parallel}) so that all data fall onto a single curve. Such a plot is shown in Fig. 5, where we have chosen $y = 0.87$. It seems to give a perfect collapse, i.e. there are no indications of any scaling violations. This might seem strange in view of the rather strong violations seen in Fig. 4. It is true that we suppressed them by plotting only data with $t > 30$, but this should not eliminate them completely. Rather,

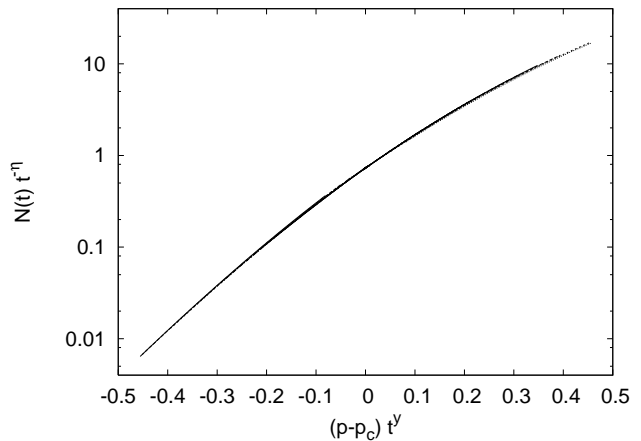


FIG. 5: Log-linear plots of $t^{-\eta}N(t)$ against $(p_c(q^*) - p)t^y$, with $q^* = 2.8$, $\eta = 0.362$, and $y = 0.87$. Only points with $t \geq 30$ are shown. Values of p range from 0.17693 to 0.185350. Notice the seemingly perfect data collapse in spite of the slightly wrong tricritical parameters and the scaling violations seen in Fig. 4.

they are not seen in Fig. 5 because of the coarse scale on the y-axis, and because we also changed slightly the tricritical parameters. We used $q^* = 2.8$ and $\eta = 0.362$, while the plot would be definitely less clean if our best estimates had been used.

A much more reliable and precise method consists in measuring $\partial N(t; q, p)/\partial p$. As we have pointed out in Sec. 2, this can be done straightforwardly. From the scaling ansatz Eq. (15) we have

$$\frac{\partial \log N(t; q^*, p_c(q^*))}{\partial p} = t^y \frac{d \log G(z)}{dz} \Big|_{z=0} \propto t^y, \quad (23)$$

up to corrections to scaling. This quantity was found to depend very weakly on the precise value of p . Thus the main uncertainty comes from its dependence on q , together with our rather large error for q^* . We plot therefore in Fig. 6 the quantity $t^{-y} \partial \log N(t)/\partial p$ for various values of q close to q^* , taking for each curve our best estimate of p_c . We see quite strong corrections to scaling (as we expected), but they do not prevent us from a very precise estimation of y . Fitting with a correction to scaling exponent $\Delta = 0.66$, i.e. with an ansatz $\partial \log N(t)/\partial p \propto t^y(1 + \text{const}/t^{0.66})$, we obtain

$$y = 0.865(3), \quad \nu_{\parallel} = 1.156(4), \quad (24)$$

and, using the previously determined value of z , $\nu_{\perp} = 0.547(3)$. Using this, we obtain also $\beta = \nu_{\parallel} \delta = 0.100(4)$ and $\beta' = \nu_{\parallel} \delta' = 1.408(10)$, where β and β' are defined via the scalings $\lim_{t \rightarrow \infty} \rho(t) \sim (p - p_c(q^*))^\beta$, $\lim_{t \rightarrow \infty} P(t) \sim (p - p_c(q^*))^{\beta'}$, both for $p > p_c$. Again these estimates, albeit being close to their mean field values, deviate from them much more than predicted by the ϵ -expansions (which is particularly simple for β' , which should be equal to $1 + O(\epsilon^2)$).

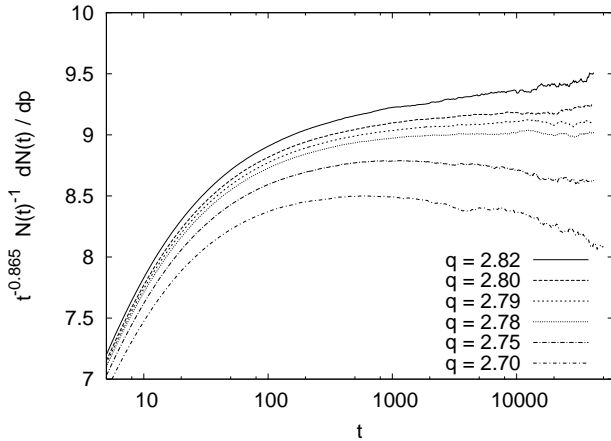


FIG. 6: Log-linear plots of $t^{-y} \partial \log N(t) / \partial p$ against t .

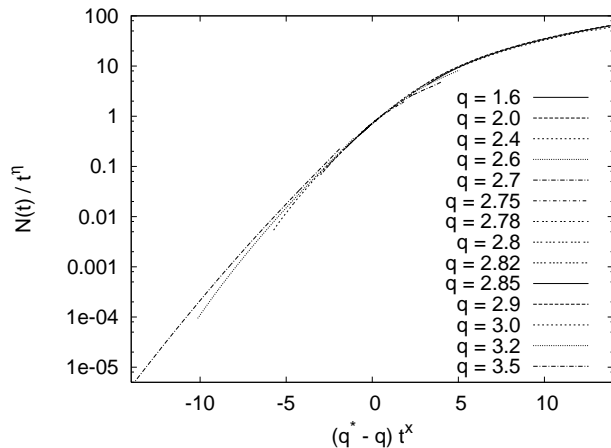


FIG. 7: Log-linear plots of $t^{-\eta} N(t; q, p_c(q))$ against $(q^* - q)t^x$, with $q^* = 2.792$, $\eta = 0.353$, and $x = 0.31$. Only points with $t \geq 24$ are shown. Values of q range from 1.6 to 3.5.

Finally, in order to measure the cross-over exponent ϕ , we can either use again a data collapse plot, or we can try to estimate the derivative of $N(t; q, p)$ (or of any other observable) along the curve $p = p_c(q)$. The latter seems however not easy. It is of course straightforward to measure the derivative in any given direction. But the orientation of the transition line $p = p_c(q)$ is only approximately known, and the derivative should depend strongly on this orientation. Thus we determined ϕ only from its data collapse, in spite of the shortcomings mentioned above.

Indeed, the situation is now much worse than in the data collapse plot for ν_{\parallel} , partly because of the uncertainties in $p_c(q)$. In Fig. 7 we show the values of $t^{-\eta} N(t; q, p_c(q))$ plotted against $(q - q^*)t^x$. The values of η and of $p_c(q)$ are as determined above, and $x = 0.31$. The data collapse is now much worse than in Fig. 5. This may be due to the fact that Eq. (14) has even larger cor-

rections to scaling than Eq. (15), but it may also be due to errors in estimating $p_c(q)$. The data collapse would improve considerably, if we would shift $p_c(q)$ for $q < q^*$ systematically towards higher values. In that case the critical curves $\ln N(t)$ versus $\ln t$ would no longer be concave, i.e. $d \ln N(t) / d \ln t$ would no longer approach approach the value $\eta_{\text{DP}} = 0.2303$ monotonically from below. Although we cannot rule out such a behaviour, we prefer to keep the estimates of $p_c(q)$ and to increase the estimated error of ϕ . We thus obtain $x = 0.31(3)$ and

$$\phi = x\nu_{\parallel} = 0.36(4). \quad (25)$$

Again the deviation from the mean field value ($\phi = 1/2$) is in the same direction as predicted by the ϵ -expansion, but is much larger in absolute value.

The numerical values of the tricritical exponents, together with the previous estimates from the ϵ -expansion and from the simulations in Ref. [10], are collected in Table 2.

D. The first order transition

As we said, data like those shown in Figs. 2,3 are strongly suggestive of stretched exponentials, but it is notoriously difficult to obtain the precise asymptotic behaviour from such curves. It seems not even clear which of the curves for $q = 3.2$ in Fig. 2 is closest to the critical one. An alternative way to obtain the critical point in this case consists in the following. We start with initial conditions where one half of the square lattice of size $L \times L$ (let us say all sites with $L/4 \leq x < 3L/4$) is active and the other half is dead. Thus we have two interfaces, at $x = L/4$ and at $x = 3L/4$ (we assume that L is a multiple of 4, and boundary conditions are periodic in the x direction). We then measure the density $\rho(x, t)$ as the system evolves. The initial step functions will become smooth sigmoidals, corresponding to fuzzy interfaces. Their positions are measured by measuring

$$X(t) = \frac{2 \sum_{x=0}^{L-1} \rho(x, t) |x - (L-1)/2|}{\sum_{x=0}^{L-1} \rho(x, t)} - L/4. \quad (26)$$

Initially, $X(t = 0) = 0$. For large t , $X(t)$ increases linearly with t if $p > p_c(q)$, while it decreases if $p < p_c(q)$.

Data for $q = 4.0$ are shown in Fig. 8, where we have plotted $\ln X(t)$ against $\ln t$ for four different values of p . In addition we show in this figure the power law $X(t) \propto t^{1/3}$ which is generically expected for a rough non-equilibrium surface which neither grows nor recedes for $t \rightarrow \infty$. We see that this is indeed the asymptotic behaviour for $p = 0.137830(3)$, which is thus our best estimate for $p_c(4.0)$.

Similar behaviour is found also for other values of $q > q^*$, except when q is very close to q^* . There the transient behaviour seen in Fig. 8 for $t < 20$ extends to much larger t , reflecting the increased internal fuzziness of the interface.

TABLE II: Estimated critical exponents for tricritical DP in 2+1 dimensions. Values for the spatial fractal dimension D_f and for the exponents γ, σ , and η_\perp not discussed in the text were obtained by means of scaling and hyperscaling relations as indicated in column #1. They are included here for easier comparison with the simulations of Ref. [10] (last column).

	defined in	present work	ϵ -expansion [5, 9]	Ref. [10]
η	Eq. (11)	-0.353(9)	$-0.0193\epsilon = -0.019$	-
δ	Eq. (11)	0.087(3)	$1/2 - 0.4677\epsilon = 0.032$	-
δ'	Eq. (11)	1.218(7)	$1 - 0.0193\epsilon = 0.981$	-
z	Eq. (11)	2.110(6)	$2 + 0.0086\epsilon = 2.009$	-
$\beta = \nu_\parallel \delta$	-	0.100(4)	$1/2 - 0.4580\epsilon = 0.042$	0.14(2)
$\beta' = \nu_\parallel \delta'$	-	1.408(10)	$1 + \mathcal{O}(\epsilon)$	-
ν_\parallel	Eq. (15) ff	1.156(4)	$1 + 0.0193\epsilon = 1.019$	-
$\nu_\perp = \nu_\parallel / z$	-	0.547(3)	$1/2 + 0.0075\epsilon = 0.507$	0.59(8)
$D_f = d - \beta/\nu_\perp$	-	1.817(8)	$2 - 0.0690\epsilon = 1.931$	1.76(5)
$\gamma = \nu_\parallel (1 + \eta)$	-	0.748(11)	$1 + \mathcal{O}(\epsilon)$	1.00(6)
$\sigma = \gamma + \beta$	-	0.848(12)	$1 - 0.0193\epsilon = 0.981$	1.12(5)
$\eta_\perp = 2 - d + 2\beta/\nu_\perp$	-	0.366(16)	$1 - 0.8620\epsilon = 0.138$	0.42(24)
ϕ	Eq. (16)	0.36(4)	$1/2 - 0.0121\epsilon = 0.488$	0.55(3)

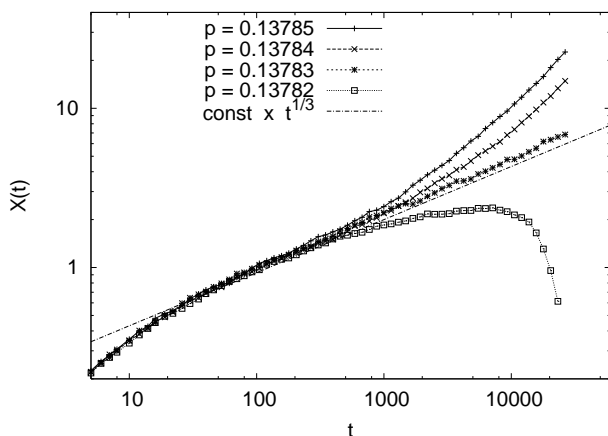


FIG. 8: Log-log plots of $X(t)$ versus t for $q = 4.0$ and four values of p . The straight line corresponds to $X(t) \propto t^{1/3}$, the generic behaviour of a non-equilibrium surface which neither grows nor recedes asymptotically.

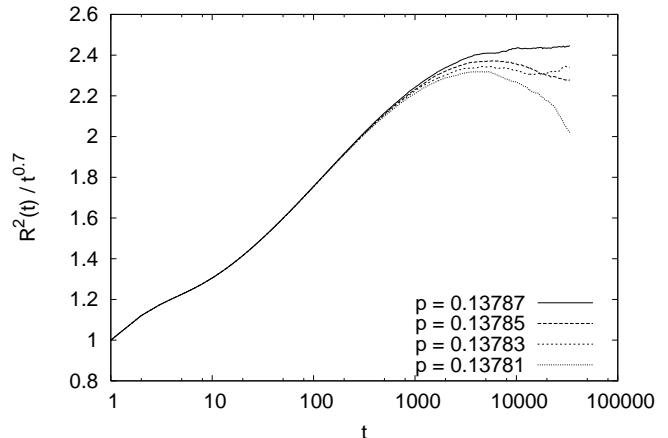


FIG. 9: Log-linear plots of $R^2(t)/t^{0.7}$ versus t , for $q = 4.0$ and four values of p .

It is an interesting question how clusters starting from a single site grow at the first order transition line. A priori one might expect the behaviour to be similar to that of a small droplet in a gas at boiling temperature, or a small domain of inverted spins in an Ising magnet at $T < T_c$. But these analogies might break down due to the essentially non-equilibrium nature of DP. Let us concentrate again on $q = 4.0$ (at other values of q , the behaviour was similar). Quantities $R^2(t)$ and $N(t)/P(t)$ (i.e., the average size of *surviving* clusters) are plotted against t in Figs. 9 and 10. Actually, in order to see the scaling more clearly, in both cases the plotted quantity was first divided by a suitable power of t , so that the curves would

be straight horizontal lines if there were pure power laws. But the curves, in particular those for the critical value $p = 0.13783$, are far from straight. They are compatible with approximate scaling laws $R^2 \sim N(t)/P(t) \sim t^{0.5}$ to $t^{0.6}$, but we are still far from the asymptotic regime. For $t \rightarrow \infty$ we should expect that surviving clusters are roughly circular and have a compact interior with density $\rho = N(t)/P(t)/R^d(t)$. If the transition is indeed first order, this density should tend to a positive constant for $t \rightarrow \infty$. As seen from Figs. 9 and 10 this is indeed the case, although this limit is reached rather late.

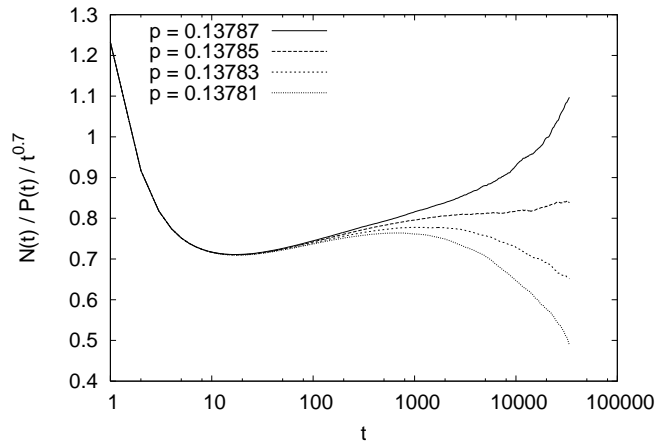


FIG. 10: Log-linear plots of $N(t)/P(t)/t^{0.7}$ versus t , for $q = 4.0$ and four values of p .

V. DISCUSSION

The main result of the present analysis is the rather poor agreement with the ϵ -expansion. This is somewhat surprising, since the upper critical dimension is $d_c = 3$ for this problem, and therefore terms linear in ϵ should give a rather good description in two dimensions. It is even more strange, since the contributions of order ϵ are extremely small for all critical exponents – except for δ , and it is only for δ that there is fairly good agreement. At least, for most exponents (except δ') the deviations from the mean field predictions have the same sign as predicted to order ϵ .

Our results are also in rather poor agreement with those of the simulations of Lübeck [10]. E.g., he found $\phi = 0.55(3)$ which is 5σ from our estimate, and which deviates from the mean field value $1/2$ in the opposite direction than the $O(\epsilon)$ term. His estimate $\nu_{\perp} = 0.59(8)$ agrees with ours within the error bars, but his estimate $\beta = 0.14(2)$ exceeds ours by 2 standard deviations. The reason for this discrepancy is not clear. It could be due to the fact that the analysis in [10] was mainly based on data collapse plots, which makes it very difficult to take into account possible corrections to scaling. As we pointed out in Sec.4.C, such plots can hide even large systematic deviations from the supposed scaling behaviour.

Overall, the simulations presented in this paper produced hardly any difficulties or surprises. Except for the data collapse for the cross-over exponent ϕ , all corrections to scaling were rather modest. We thus believe that our analysis is robust and does not hide any large systematic errors.

This is in marked contrast to the PCPD [7], which can be viewed as an alternative tricritical version of standard DP. It would be nice to have a model where the PCPD arises as a singular limit of TDP. The version of the generalized Domany-Kinzel model which we used in the present paper does not give rise to the PCPD in any

limit.

After having discussed tricritical directed percolation, we should mention also tricritical ordinary (undirected) percolation. A field theoretic renormalization treatment of this problem has been given recently by Janssen and coworkers [6]. Discrete lattice model versions can be formulated in close analogy to the present work. Let us consider the dynamic version, i.e. the generalized epidemic process (GEP) [31]. This is very similar to directed percolation viewed as an epidemic process, except that lattice sites which had once been infected cannot be reinfected again (this is also known as the SIR model, for “susceptible-infected-removed”). In a generalized GEP (GGEP) one can modify the probabilities P_k to be infected by k infectious neighbours in the same way as we did in the present paper (Eq. 5), but one can also use other Ansätze for P_k with the same qualitative behaviour. Typically, a tricritical regime is reached when P_k increases sufficiently fast with k . Models of this type were studied some time ago by Cieplak, Robbins, Koiller and others [32]. A comparison of their results with the theoretical work of [6] would be very welcome. Also, there are some surprising claims in [32], e.g. it is claimed in some of these papers that there is also a transition between pinned fractal (i.e. percolation like) clusters and compact clusters with self-affine surfaces in 1+1 dimensions. One should expect such a transition to occur in higher dimensions, but like the transition to compact DP in the 2-d Domany-Kinzel model, it should occur in 1+1 dimensions only at the boundary of the control parameter space.

Finally, it is instructive to compare different epidemic models, and we shall finish this paper with a short review of how the different schematic models discussed in the literature are related. Let us first assume we can have three different types of individua in a population: Healthy susceptible ones (S), ill and infective ones (X), and “removed” individua (R), which might either mean immune or dead. Then we have the following basic schemes:

- The only reaction is $S + X \rightarrow X + X$, i.e. ill individua remain infective forever. This gives Eden growth [18].
- In addition we have $X \rightarrow R$, i.e. ill individua have a finite life time and are removed thereafter. This gives the GEP.
- Instead of $X \rightarrow R$ we have $X \rightarrow S$, i.e. after individua have recovered they become again susceptible. This gives DP.
- If we add a reaction $R \rightarrow S$ to the GEP, it should bring the model into the DP universality class, except when the rate of this last reaction is very small. In the limit when this rate is much smaller than all other rates, we obtain the Bak-Chen-Tang [33] forest fire model.

If we have in addition a fourth class (W) of individua weakened by the contact with an infective, but neither ill nor infective themselves, then we get three more schemes:

- If we change the recovery in DP to $X \rightarrow W$ and add $W + X \rightarrow X + X$, i.e. recovered individua have a different chance to be re-infected by a subsequent contact with ill ones, we obtain the model of Grassberger, Chaté, and Rousseau [15]. Notice that in this model weakened individua stay weak forever, and never regain their strength.
- If we include in addition the reaction $W \rightarrow S$, then weakening is only transient and we should expect to be again in DP.
- If, however, transient weakening happens not *after* but *instead of* an infection, i.e. if we add $S + X \rightarrow W + X$, $W + X \rightarrow X + X$, and $W \rightarrow S$ to DP, we obtain the model discussed in the present paper.
- If we add $S + X \rightarrow W + X$ and $W + X \rightarrow X + X$

(but not $W \rightarrow S$) to the GEP, we end up at the GGEP.

Obviously this list is not exhaustive. It seems however to contain all interesting cases, if we assume that the reservoir of susceptible individua is unlimited (conservation of the total population size is irrelevant), and that there is some local saturation mechanism which prevents any of the densities to explode. Whether this is indeed true, or whether there exist more such models with interesting novel behaviour, is still an open question.

Acknowledgements:

I am indebted to Sven Lübeck for showing me his results prior to publication, without which I would not have started this work. I also want to thank Maya Paczuski for several discussions, and I want to acknowledge the hospitality of the Perimeter Institute where this work was started. Finally I want to Hannes Janssen and Sven Lübeck for several critical e-mails and for carefully reading the paper.

-
- [1] M. Moshe, Phys. Rep. C **37**, 225 (1978).
 [2] P. Grassberger and K. Sundermeyer, Phys. Lett **77B**, 220 (1978).
 [3] P. Grassberger, Z. Phys. B **47**, 365 (1982).
 [4] H.-K. Janssen, J. Phys. A: Math. Gen. **20**, 5733 (1987).
 [5] T. Ohtsuki and T. Keyes, Phys. Rev. A **35**, 2697; **36**, 4434 (1987)
 [6] H.-K. Janssen, M. Müller, and O. Stenull, Phys. Rev. E **70**, 026114 (2004).
 [7] M. Henkel and H. Hinrichsen, J. Phys. A **37**, R117 (2004).
 [8] H.-K. Janssen, F. Wijland, O. Deloubrière, and U.C. Täuber, Phys. Rev. E **70**, 056114 (2004).
 [9] H.-K. Janssen, J. Phys.: Cond. mat. **17**, S1973 (2005).
 [10] S. Lübeck, preprint (2005).
 [11] H. Hinrichsen, Adv. Phys. **49**, 815 (2000).
 [12] E. Domany and W. Kinzel, Phys. Rev. Lett. **53**, 311 (1984).
 [13] J.W. Essam, J. Phys. A **22**, 4927 (1989).
 [14] For general arguments why first order transitions are not possible in 1+1 dimensional models of this type, see H. Hinrichsen, cond-mat/0006212.
 [15] P. Grassberger, H. Chaté, and G. Rousseau, Phys. Rev. E **55**, 2488 (1997).
 [16] A. Jimenez-Dalmaroni and H. Hinrichsen, Phys. Rev. E **68**, 036103 (2003).
 [17] In both models, it is easier for an epidemic to survive in a region, than to spread out into new regions. While this happens by an explicit long time memory effect in the GCR model (sites which were once infected are more easily re-infected), it happens in the present model because sites inside an infected region have more infected neighbours than sites on the outer boundary. In both cases, a critical cluster grows slower than in ordinary DP, and thus has a larger chance to die due to random fluctuations.
 [18] M. Kardar, G. Parisi, and Y.-C. Zhang, Phys. Rev. Lett. **56**, 889 (1986).
 [19] P. Grassberger, Phys. Rev. E **56**, 3682 (1997).
 [20] R. Dickman, Phys. Rev. E **60**, R2441 (1999).
 [21] H.G. Ballesteros *et al.*, Phys. Lett. B **400**, 346 (1997).
 [22] P. Grassberger, Phys. Rev. E **67**, 036101 (2003).
 [23] P. Grassberger and A. de la Torre, Ann. Phys. (N.Y.) **122**, 373 (1979).
 [24] P. Grassberger and Y.-C. Zhang, Physica A **224**, 169 (1996).
 [25] E. Perlsman and S. Havlin, Europhys. Lett. **58**, 176 (2002).
 [26] J.F.F. Mendes, R. Dickman, M. Henkel, and M.C. Marques, J. Phys. A **27**, 3019 (1994).
 [27] Eq.(15) holds indeed on any smooth curve in the (p, q) -plane which cuts the transition curve transversally in the tricritical point, not only for the vertical line $q = q^* = \text{const}$.
 [28] C.A. Voigt and R.M. Ziff, Phys. Rev. E **56**, R6241 (1997).
 [29] F. Schlögl, Z. Phys. **253**, 147 (1972).
 [30] R.M. Ziff and B.J. Brosilow, Phys. Rev. A **46**, 4630 (1992).
 [31] P. Grassberger, Math. Biosci. **63**, 157 (1983).
 [32] M. Cieplak and M.O. Robbins, Phys. Rev. Lett. **60**, 2042 (1988); Phys. Rev. B **41**, 11508 (1990); N. Martys, M. Cieplak, and M.O. Robbins, Phys. Rev. Lett. **66**, 1058 (1991); N. Martys, M.O. Robbins, and M. Cieplak, Phys. Rev. B **44**, 12294 (1991); B. Koiller, H. Ji, and M.O. Robbins, Phys. Rev. B **45**, 7762 (1992); **46**, 5258 (1992); C.S. Nolle, B. Koiller, N. Martys, and M.O. Robbins, Phys. Rev. Lett. **71**, 2074 (1993); B. Koiller and M.O. Robbins, Phys. Rev. B **62**, 5771 (2000).
 [33] P. Bak, K. Chen, and C. Tang, Phys. Lett. A, **147**, 297 (1990).